

Silica Precipitation in Fractures and the Evolution of Permeability in Hydrothermal Upflow Zones

Robert P. Lowell, Philippe Van Cappellen,
Leonid N. Germanovich

Analytical models are used to compare the rates at which an isolated fracture and vertical, parallel fracture sets in hydrothermal upflow zones can be closed by silica precipitation and thermoelastic stress. Thermoelastic sealing is an order of magnitude faster than sealing by silica precipitation. In vertical fracture sets, both the amount of silica precipitation resulting from cooling and the total thermal expansion of the country rock may be insufficient to seal cracks at depth. These crack systems may ultimately close because the pressure dependence of silica solubility maintains precipitation during upflow even after the temperature gradient vanishes.

Rock permeability controls fluid circulation in hydrothermal systems (1). This highly variable parameter ranges from $\sim 10^{-10}$ m² in fractured igneous and metamorphic rocks to $\sim 10^{-20}$ m² in unfractured rocks (2). Estimates of mean permeability in hydrothermal systems tend to range between 10^{-11} and 10^{-16} m² (3), which indicates that, in these environments, the permeability mainly arises from fractures. Moreover, the permeability may vary both spatially and temporally in response to tectonic and thermal stress as well as to chemical dissolution and precipitation (4–7). An understanding of the evolution of a hydrothermal system thus requires knowledge of how fracture-controlled permeability evolves in space and time.

In this report, we investigate crack closure resulting from silica precipitation in hydrothermal upflow zones that occurs in response to the decrease in solubility of solid SiO₂ phases upon cooling and decompression of the ascending fluids (8). We consider the idealized cases of a single fracture and a set of planar, parallel, and vertical fractures (Fig. 1). We obtain analytical formulas for the fracture width as a function of time and compare the rate of fracture closure resulting from silica precipitation with that resulting from thermoelastic stresses (6). We also explain the formation of a thin surficial crust observed at a hydrothermal site along the northern Gorda Ridge. Moreover, the analytical solutions can be used to check numerical models of fracture closure.

Recent studies of chemical reactions between hydrothermal solutions and the surrounding rock (9) follow from the seminal work of Helgeson (10). Wood and Hewett (11), Walder and Nur (12), and

Wells and Ghiorso (13) have attempted to show how porosity and permeability are reduced as a result of silica precipitation in hydrothermal systems. Chemical equilibrium between silica and the fluid was assumed in (11) and (12); a linear precipitation-rate law was used in (13). In each of these studies, a uniform Darcian flow in a porous medium and a constant geothermal gradient were assumed. These studies illustrate the importance of the average fluid velocity, which determines the flux of silica to the site of deposition, and the temperature gradient, which controls the rate of silica precipitation; however, a temperature gradient that is constant in space and time is not realistic for a hydrothermal system. Similarly, fracture-controlled flow dominates rather than Darcian flow.

For a single fracture of width b and constant length in an impermeable medium, the mass balance of silica entering at position x and leaving at $x + dx$ is given by

$$\rho_s \frac{\partial b}{\partial t} = q \frac{\partial c_s}{\partial x} \quad (1)$$

where $\rho_s = 2.5 \times 10^3$ kg m⁻³ is the density of silica, t is time, $q = \rho_f v b$ is the mass flow rate of fluid, $\rho_f = 10^3$ kg m⁻³ is the density of water, v is the velocity of

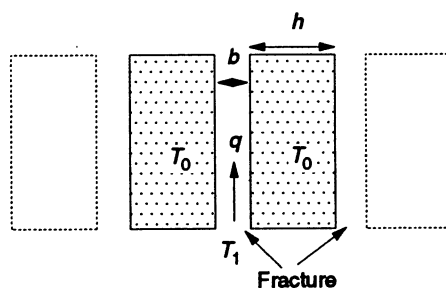


Fig. 1. Schematic drawing showing fluid upflow at mass flow rate q in a fracture of width b . The rock temperature is initially T_0 , and the fluid temperature at the inlet is T_1 . For treatment of a single fracture, the fracture spacing h is set at infinity.

fluid in the fracture, and c_s is the mass concentration of silica in solution (kg/kg). The left side represents the growth rate of quartz per unit surface area of the fracture wall. The equation shows, therefore, that the dissolved silica gradient ($\partial c_s / \partial x$) is determined by the mass flow of fluid and the precipitation kinetics of quartz. The gradient vanishes for high fluid velocities, large fracture widths, and slow kinetics. We have neglected the dispersion of silica along the fracture and diffusion of silica into the country rock. We have also neglected other possible mineral precipitation or dissolution reactions. These processes could be included in more complete models.

The precipitation rate is driven by the degree of supersaturation of the fluid with respect to silica. Because silica solubility depends on temperature T and pressure P , it is useful to write

$$\frac{\partial c_s}{\partial x} = \frac{\partial c_s}{\partial T} \frac{\partial T}{\partial x} + \frac{\partial c_s}{\partial P} \frac{\partial P}{\partial x} \quad (2)$$

The pressure gradient can be approximated by the hydrostatic gradient $-\rho_f g$, where g is the acceleration of gravity. The minus sign occurs because x is defined positive upwards.

To calculate $\partial T / \partial x$, we consider the opening of a fracture of width b_0 at time $t = 0$ in rock initially at temperature T_0 . Fluid enters the crack at $x = 0$ and flows through the crack at a mass flow rate q per unit length of the fracture (Fig. 1). The heat transported by fluid flowing in the fracture is equal to the rate at which heat is conducted into the rock. The temperatures of the fluid and rock at the fracture-rock interface are assumed to be equal. At $x = 0$, the fluid is maintained at a constant temperature T_1 . Then, after an initial, short-lived transient, the temperature of the fluid in the fracture is (14):

$$T(x, t) = T_0 + (T_1 - T_0) \operatorname{erfc} \left(\frac{\lambda x}{sq \sqrt{at}} \right) \quad (3)$$

where erfc is the complementary error function, $\lambda = 2.5$ W m⁻¹ °C⁻¹ is the thermal conductivity of rock, $s = 4 \times 10^3$ J kg⁻¹ °C⁻¹ is the specific heat of the fluid, and $a = 10^{-6}$ m² s⁻¹ is the thermal diffusivity of rock. Substituting $\partial T / \partial x$ from Eq. 3 into Eq. 2 and inserting the result in Eq. 1, we get

$$\frac{\partial b}{\partial t} = - \frac{2\lambda(T_1 - T_0)}{\rho_s s \sqrt{\pi a t}} \frac{\partial c_s}{\partial T} \exp \left[- \left(\frac{\lambda x}{sq \sqrt{at}} \right)^2 \right] - \frac{q \rho_f g}{\rho_s} \frac{\partial c_s}{\partial P} \quad (4)$$

Integration of Eq. 4, with $b = b_0$ at $t = 0$ yields

R. P. Lowell and P. Van Cappellen, School of Earth and Atmospheric Sciences, Georgia Institute of Technology, Atlanta, GA 30332.

L. N. Germanovich, School of Petroleum and Geological Engineering, University of Oklahoma, Norman, OK 73019.

$$b(x,t) = b_0 - \left[\frac{2\lambda(T_1 - T_0)}{\rho_s s \sqrt{\pi a}} \frac{\partial c_s}{\partial T} \right] \left[2\sqrt{t} \exp\left(\frac{-\lambda^2 x^2}{s^2 q^2 a t}\right) - \frac{2\lambda x}{sq} \sqrt{\frac{\pi}{a}} \operatorname{erfc}\left(\frac{\lambda x}{sq \sqrt{\pi a}}\right) \right] - \frac{q\rho_f g}{\rho_s} \frac{\partial c_s}{\partial P} t \quad (5)$$

Equation 5 shows that $b(x,t)$ decreases most rapidly at the inlet to the fracture, $x = 0$, where

$$b(0,t) = b_0 - A(T_1 - T_0)t^{1/2} - Bqt \quad (6)$$

where $A = [4\lambda/\sqrt{\pi a} \rho_s s][\partial c_s/\partial T]$ and $B = [\rho_f g/\rho_s][\partial c_s/\partial P]$.

To calculate the closure time of a fracture with Eq. 6, we need estimates for $\partial c_s/\partial T$ and $\partial c_s/\partial P$. When the precipitation kinetics are fast relative to the rate of fluid advection, silica precipitation is able to maintain the fluid composition close to equilibrium, and $\partial c_s/\partial T$ and $\partial c_s/\partial P$ may be approximated by the temperature and pressure derivatives, respectively, of silica solubility. In general, the assumption of local chemical equilibrium provides an upper bound on model calculations that are based on experimentally determined kinetics of silica precipitation.

Using silica solubility data from Fournier (8) in a solution with 0.51 m NaCl between 200° and 300°C, we find $\partial c_s/\partial T \approx 6 \times 10^{-6} \text{ K}^{-1}$. The solubility of silica in pure water as a function of pressure (15) yields $\partial c_s/\partial P \approx 10^{-12} \text{ Pa}^{-1}$ if $T \leq 300^\circ\text{C}$; at $T > 300^\circ\text{C}$ and $P > 200$ bars, $\partial c_s/\partial P \approx 10^{-11} \text{ Pa}^{-1}$. This approach gives $A = 2.8 \times 10^{-9} \text{ m s}^{-1/2} \text{ }^\circ\text{C}^{-1}$ and $B = 4 \times 10^{-12} \text{ m}^2 \text{ kg}^{-1}$ for $T \leq 300^\circ\text{C}$. For a temperature difference of 100°C, Eq. 6 gives about 0.4 year as the shortest time for the closure of a 1-mm-wide fracture. This result is not very sensitive to the flow rate for $q \leq 0.1 \text{ kg m}^{-1} \text{ s}^{-1}$, which indicates that the temperature-gradient term in Eq. 6 is more important than the pressure-gradient term for large temperature differences. For a temperature difference of 10°C, the time to close a 1-mm-wide fracture according to Eq. 6 is about 20 years for $q = 0.1 \text{ kg m}^{-1} \text{ s}^{-1}$, or 40 years for $q = 0.01 \text{ kg m}^{-1} \text{ s}^{-1}$. Thus, for small temperature differences between the fluid and the rock, the effect of pressure on solubility can be a significant driving force for precipitation.

The above result holds for constant q . The average mass flow per unit length of the fracture is related to the pressure head H driving the flow by $q = (b^3/12\nu)H$, where ν is the kinematic viscosity of water, ranging from 10^{-6} to $10^{-7} \text{ m}^2 \text{ s}^{-1}$. Thus, if the head remains constant, q will decrease as b decreases. The term that involves the effect of pressure on solubility

in Eq. 6 will decrease as the flow decreases. The term that involves the effect of temperature on solubility is more complicated. The temperature distribution (Eq. 3) is for constant q ; however, this equation was derived from the balance between heat advected by fluid flowing in the fracture, $q\partial T/\partial x$, and heat conducted into the adjacent country rock. Because heat conduction is proportional to $t^{-1/2}$, this time dependence also holds for $q\partial T/\partial x$. This result, combined with Eqs. 1 and 2, implies that the second term on the right side of Eq. 6 should still be proportional to $t^{1/2}$ even though q decreases with time. In any case, Eq. 6 holds for the early stages of crack closure by silica precipitation, provided the kinetics are fast.

Equation 6 can be compared directly with the equation for closure of a single fracture by thermoelastic stresses. If the wall of a single crack of initial width b_0 is maintained at temperature T_1 in an infinite medium at initial temperature T_0 , where $T_1 > T_0$, the crack faces will be displaced inward as a result of the thermal expansion of the adjacent rock. The crack width is given by (6, 16)

$$b(t) = b_0 - \frac{20\alpha_r}{9} (T_1 - T_0) \sqrt{\frac{at}{\pi}} \quad (7)$$

where $\alpha_r = 10^{-5} \text{ }^\circ\text{C}^{-1}$ is the thermal expansion coefficient for rock. Comparison of Eqs. 6 and 7 shows that the temporal dependence for thermal and chemical sealing is identical. Substitution of typical values, however, yields a numerical factor governing the rate of fractional closure $(b_0 - b)/b_0$ that is about an order of magnitude greater for thermal than for chemical sealing. Thus, for a single fracture, the calculations suggest that permeability changes induced by thermal stress and by silica precipitation operate on different time scales.

Suppose a fracture is closing as a result of simultaneous thermal expansion and silica precipitation. Because thermal expansion occurs about ten times faster than silica precipitation, only a relatively thin layer of silica will exist when the fracture is closed. Thus, a thin silica-filled vein may have initially been a much wider fracture. Moreover, after the fracture is sealed, the rock would tend to cool because the hot hydrothermal fluid is no longer able to flow through it. Thermoelastic stress would then tend to reopen the fracture, but this may be rendered more difficult because of the chemical sealing of the fracture. Coupled thermoelastic and chemical effects may lead to oscillatory behavior, which may explain why in fractures there are numerous generations of silica.

Now consider a set of planar, parallel, and vertical fractures of initial width b_0 that are separated by a distance h (Fig. 1). In this case, thermal interference between the fractures will limit the amount of closure that can occur by either the thermal expansion or chemical precipitation that results from the temperature gradient along the fracture. The mass balance for silica in an individual fracture is the same as for a single fracture, but the thermal problem is different because there is no heat flux across the midplane between adjacent fractures. We consider a uniform flow rate q per unit length in each fracture in an infinite number of fractures. The fluid enters at $x = 0$ at temperature T_1 , and the rock is assumed to be initially at temperature T_0 . This thermal problem can be solved in Laplace transform space (17). Substitution of Eq. 2 into Eq. 1 and integration with respect to time yields

$$b(x,t) = b_0 + \frac{q}{\rho_s} \frac{\partial c_s}{\partial T} \int_0^t \frac{\partial T}{\partial x} dt - \frac{\rho_f g q}{\rho_s} \frac{\partial c_s}{\partial P} t \quad (8)$$

Maximum closure caused by precipitation along the temperature gradient is found with the solution of Eq. 8 in the limit as $t \rightarrow \infty$ and $x \rightarrow 0$, with $\partial c_s/\partial P = 0$. Application of well-known theorems from Laplace transforms to the solution provided by Gringarten *et al.* (17) for $\partial T/\partial x$ in this limiting case gives (18)

$$b(0, \infty) = \lim_{p \rightarrow 0} [pb^*(x,p)] = b_0 - (T_1 - T_0) \frac{h\rho_r c_r}{\rho_s} \frac{\partial c_s}{\partial T} \quad (9)$$

where $b^*(x,p)$ is the Laplace transform of $b(x,t)$, ρ_r is the density of country rock, and $c_r = 10^3 \text{ J kg}^{-1} \text{ }^\circ\text{C}^{-1}$ is the specific heat of rock. This result can be compared directly with the maximum thermoelastic closure for a set of parallel fractures (6)

$$b(\infty) = b_0 - (T_1 - T_0) \frac{5\alpha_r h}{9} \quad (10)$$

Substitution of parameter values for comparison of Eqs. 9 and 10 indicates that the total closure attributable to thermal expansion is about three times that resulting from precipitation driven by the temperature dependence of silica solubility.

In the derivation of Eq. 9, the effect of pressure was neglected. However, the dependence of silica solubility on pressure may lead to continued silica precipitation even after the temperature gradient vanishes. When $\partial T/\partial x \rightarrow 0$, the last term on the right side of Eq. 8 controls the fracture width. This term is valid only if q is constant, and q is expected to decrease with time, as discussed above. As long as q is finite, however, the fracture width will continue to decrease because of the persistence of the hydrostatic pressure gradient.

Finally, consider the formation of a thin, impermeable crust at the sea floor as a result of silica precipitation in a fracture set during hydrothermal discharge. An example may be found at the Sea Cliff hydrothermal field on the northern Gorda Ridge in the northeast Pacific Ocean (19). This field contains an area at least 50 m by 100 m that is capped by an irregular crust several centimeters thick, which is in part cemented by silica.

In this problem, we consider a quasi-steady-state situation in which the temperature profile results from uniform upflow of fluid through a set of parallel vertical fractures of width b and separation h . At depth, the temperature is $T = T_1$; at the sea-floor boundary, $T = 0^\circ\text{C}$. This problem can be interpreted to be the steady-state result for upflow through a fracture set (Fig. 1). The temperature of the fluid in the cracks is now in equilibrium with the adjacent rock, and all thermoelastic expansion and chemical precipitation at depth in the fracture system has taken place.

The upflow velocity in each crack, v , can be written in terms of a Darcian velocity $v_d = \phi v$, where $\phi = b/h$ is the porosity. The temperature distribution $T(x)$ is given by:

$$T(x) = T_1[1 - \exp(-v_d x/a^*)] \quad (11)$$

where $a^* = \lambda/\rho_f s$ is the effective thermal

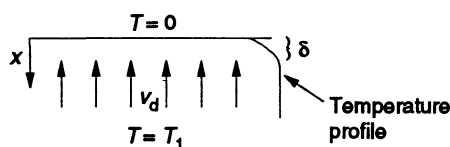


Fig. 2. Uniform Darcian upflow at velocity v_d and temperature T_1 at depth. On the right of the diagram is the temperature profile, which shows the conductive thermal boundary layer of thickness δ .

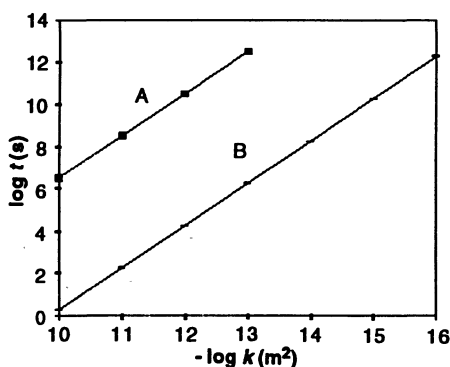


Fig. 3. Time to close fractures of initial width b_0 and separation h in the near-surface boundary layer of width δ for the Darcian convective-upflow problem as a function of bulk permeability k . Curve A is for $T_1 = 50^\circ\text{C}$, $\nu = 10^{-6} \text{ m}^2 \text{ s}^{-1}$, and $\alpha = 10^{-4} \text{ }^\circ\text{C}^{-1}$; curve B is for $T_1 = 300^\circ\text{C}$, $\nu = 10^{-7} \text{ m}^2 \text{ s}^{-1}$, and $\alpha = 10^{-3} \text{ }^\circ\text{C}^{-1}$.

diffusivity and x is now positive downward from the surface. For typical values of v_d , the temperature distribution given by Eq. 11 remains close to T_1 , except in a thin thermal boundary layer of thickness $\delta \approx a^*/v_d$, within which conduction to the surface is important (Fig. 2). Chemical precipitation will be concentrated in this boundary layer where the temperature decreases sharply. In this region, crack closure by thermal expansion is relatively unimportant because the temperature is low; the pressure effect on solubility can also be neglected because the temperature gradient is large. The temperature gradient is greatest at $x = 0$, where $dT/dx = T_1 v_d/a^*$. Substitution of this value for dT/dx into Eq. 2 and insertion of Eq. 2 into Eq. 1 yields

$$\frac{db}{dt} = -\frac{\partial c_s}{\partial T} \frac{\rho_f T_1 h v_d^2}{\rho_s a^*} \quad (12)$$

where q in Eq. 1 has been replaced by $\rho_f b v_d / \phi$.

The upward Darcian velocity v_d is assumed to result from buoyancy forces between cold, downward-circulating fluid and the hot, ascending fluid. Thus

$$v_d \approx g \alpha k T_1 / \nu \quad (13)$$

where α is the thermal expansion coefficient for water, which ranges from 10^{-4} to $10^{-3} \text{ }^\circ\text{C}^{-1}$. Because precipitation takes place mainly in the boundary layer, we can assume that the bulk permeability, k , remains constant as the uppermost layer of the crust is sealed by chemical precipitation. Substituting Eq. 13 into Eq. 12 and integrating, we get

$$\frac{b(t)}{b_0} = 1 - \frac{\rho_f T_1^3}{\rho_s a^* \phi_0} \left(\frac{k \alpha g}{\nu} \right)^2 \frac{\partial c_s}{\partial T} t \quad (14)$$

where ϕ_0 is the initial porosity b_0/h .

The fracture width $b(t)$ depends strongly on a number of parameters that themselves are highly variable (for example, k^2 dependence); therefore, the time to close a given fracture by quartz deposition can vary over many orders of magnitude (Fig. 3). The results for $T_1 = 50^\circ\text{C}$ are similar to those in (11). For $T_1 = 300^\circ\text{C}$, however, the time for crack sealing is many orders of magnitude faster. This is, in part, because of the relatively high value of α/ν in high-temperature systems. The calculated closure times for the low-temperature situation are underestimates because, at temperatures below 100°C , the precipitation rate of silica becomes very slow, and it is unlikely that saturation with quartz is maintained (8).

When the Alvin temperature probe was inserted into the impermeable crust at the Sea Cliff hydrothermal field on the northern Gorda Ridge, the temperature immediately registered 94°C at a depth of 5 cm

(19). If this crust is underlain by water upflowing at 350°C , the observed temperature at 5 cm, together with Eq. 11, yields an upward velocity $v_d = 2 \times 10^{-6} \text{ m s}^{-1}$. Substitution into Eq. 13 gives a permeability $k \approx 6 \times 10^{-14} \text{ m}^2$. According to the results in Fig. 3, the crust could be effectively sealed within less than a decade.

The calculations in this report suggest that permeability in hydrothermal upflow zones may be significantly modified by the precipitation of silica on relatively short time scales. In the deeper parts of hydrothermal systems, however, fracture closure as a result of silica precipitation does not appear to occur as rapidly as thermoelastic closure.

REFERENCES AND NOTES

1. R. P. Lowell, *Rev. Geophys.* **29**, 457 (1991).
2. W. F. Brace, *Int. J. Rock Mech. Min. Sci.* **17**, 241 (1980); *J. Geophys. Res.* **89**, 4327 (1984).
3. For example, J. R. Cann and M. R. Strens, *J. Geophys. Res.* **94**, 12227 (1989); R. P. Lowell and D. K. Burnell, *Earth Planet. Sci. Lett.* **104**, 59 (1991); D. Norton and H. P. Taylor, *J. Petrol.* **20**, 421 (1979).
4. D. E. White, M. W. Brannock, K. J. Murata, *Geochim. Cosmochim. Acta* **10**, 27 (1956); R. O. Fournier, in *Reviews in Economic Geology*, B. R. Berger and P. M. Bethke, Eds. (Society of Economic Geologists, El Paso, TX, 1985), vol. 2, pp. 45-62.
5. For example, R. O. Fournier, *U.S. Geol. Surv. Prof. Pap.* **350** (1987), p. 1487.
6. R. P. Lowell, *Geophys. Res. Lett.* **17**, 709 (1990).
7. L. N. Germanovich and R. P. Lowell, *Science* **255**, 1564 (1992).
8. R. O. Fournier, *Geochim. Cosmochim. Acta* **47**, 579 (1983).
9. For example, A. C. Lasaga, *J. Geophys. Res.* **89**, 4009 (1984); P. C. Lichtner, *Geochim. Cosmochim. Acta* **49**, 779 (1985); *ibid.* **52**, 143 (1988); C. I. Steefel, thesis, Yale University (1992).
10. H. C. Helgeson, *Geochim. Cosmochim. Acta* **32**, 853 (1968); in *Geochemistry of Hydrothermal Ore Deposits*, H. L. Barnes, Ed. (Wiley, New York, 1979), pp. 568-610.
11. J. R. Wood and T. A. Hewett, *Geochim. Cosmochim. Acta* **46**, 1707 (1982).
12. J. Walder and A. Nur, *J. Geophys. Res.* **89**, 11539 (1984).
13. J. T. Wells and M. S. Ghiorso, *Geochim. Cosmochim. Acta* **55**, 2467 (1991).
14. G. Bodvarsson, *J. Geophys. Res.* **74**, 1987 (1969); R. P. Lowell, *ibid.* **81**, 359 (1976).
15. G. C. Kennedy, *Econ. Geol.* **45**, 629 (1950); R. O. Fournier and R. W. Potter II, *Geochim. Cosmochim. Acta* **46**, 1969 (1982).
16. G. Bodvarsson, in *Proceedings of the 2nd United Nations Symposium on the Development and Use of Geothermal Resources* (Government Printing Office, Washington, DC, 1975), pp. 903-907.
17. A. C. Gringarten, P. A. Witherspoon, Y. Onishi, *J. Geophys. Res.* **80**, 1120 (1975); E. S. Romm, *Problemy Razrabotki Mestorozhdenii Poleznykh Iskopaemykh Severa* (Leningrad Mining Institute, Leningrad, 1972).
18. We have corrected a small error in the solution provided by Gringarten *et al.* (17).
19. P. A. Rona *et al.*, *Geology* **18**, 493 (1990).
20. We thank C. Steefel and an anonymous reviewer for helpful comments on a earlier version of this manuscript. This work was supported by the NSF under grants OCE 9012665 and OCE 9216976 to R.P.L. and OCE 9221349 to L.N.G.

23 November 1992; accepted 18 February 1993